Load carrying capacity of masonry bridges: numerical evaluation of the influence of fill and spandrels

A. Cavicchi and L. Gambarotta
Department of Structural and Geotechnical Engineering, University of Genova, Italy

ABSTRACT. The contribution of arch-fill interaction to the load carrying capacity of masonry bridges can be large [1]. While a comprehensive description of arch-fill-spandrels interaction requires a three-dimensional model, a simplified description of fill contribution to the load carrying capacity of the bridge can be implemented in two-dimensional models. This is the way followed for instance in Hughes *et al.*[2] and by Bicanić *et al.* [3]. In Cavicchi and Gambarotta [4] fill is described as a continuum in plane strain. This reduction of fill to a plane model presents a critical aspect whose effects have to be evaluated: the dependence of the in-plane fill resistance on the containing capacity of the spandrels. This aspect is here considered in an approximated way by describing fill as a continuum in a plane state where the out of plane normal stress is constrained in an admissible domain representing the limited containing action of the spandrels. A statically admissible two-dimensional model is defined and the Static Theorem of Limit Analysis is applied.

1. INTRODUCTION

One of the most relevant problem in the assessment of masonry bridges is the evaluation of the load carrying capacity including the strengthening effect of fill interacting with spandrel walls. This circumstance has been highlighted by experimental collapse tests on full scale and model scale bridges [1].

Even if a comprehensive analysis of the interaction between arch, fill and spandrels would call for detailed three-dimensional models [2], in some cases, when transverse effects can be neglected and spandrel walls are not considered, the structural system can be described by a plane model. This makes it possible to assume simplified constitutive models for masonry, thereby reducing the sources of uncertainties; moreover, the bridge behaviour can be more synthetically described. Two-dimensional models based on the no-tension assumption for masonry, originally proposed in the pioneering works by Castigliano [3], Kooharian [4] and Heyman [5], have been extended by various authors to take into account fill ([6]-[10]). Cavicchi [11] and Cavicchi and Gambarotta [12-13] have proposed a model in which the fill is described as a cohesive-frictional continuum interacting with the arch-pier system represented by no-tension, perfectly plastic beams; upper estimates of the collapse load and the corresponding collapse mechanisms have been obtained. The unconservative nature of the results from the kinematic approach may represent a problem.

Aim of this paper is to overcome this limitation by applying the lower bound theorem of limit analysis to a statically admissible FE discretization of the mechanical model defined in Cavicchi and Gambarotta [13] and take into account the effects of a limited transverse constraining action of the spandrel walls on the fill by introducing a condition which limits the transverse compressive stress under an admissible value; this feature provides a simplified

means to evaluate the dependence of the collapse load on the transverse effects and release and discuss the plane strain assumption [14].

2. PLANE EQUILIBRIUM MODEL OF THE ARCH BRIDGE

A longitudinal cross section of a typical masonry bridge is diagrammatically described in Figure 1.a; the structural model described in Figure 1.b is assumed, in which the spandrel walls are not considered. The volume occupied by fill is represented by the two-dimensional domain Ω_f, corresponding to a longitudinal section of fill, while arch barrels and piers are described by plane curved beams. The piers at the base and the arch barrels at springings are considered built in and the connections between the arch springings and the top of the piers are assumed rigid. The fill is restrained at the opposite ends of the bridge.

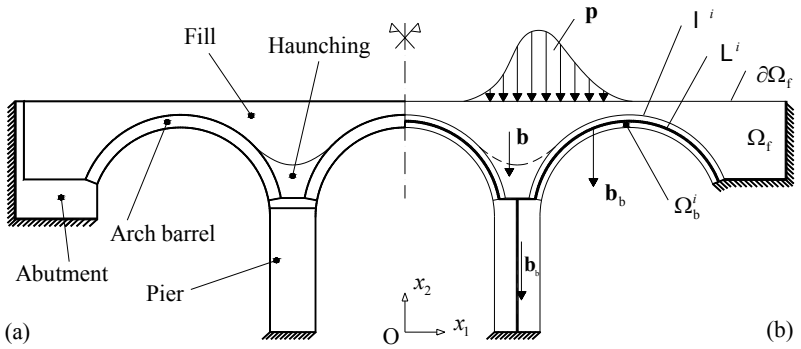

Fig. 1. (a) Longitudinal cross section and (b) two-dimensional model of the bridge.

The external forces, represented by self weight $\mathbf{b}$ and the line tractions $\mathbf{p}$ over the upper boundary of the fill, are assumed parallel to the plane of the longitudinal cross section of the bridge and uniform across the width.. The load vector $\mathbf{p}$ is decomposed as $\mathbf{p}=\mathbf{p}_0+s\bar{\mathbf{p}}$, where $\mathbf{p}_0$ is fixed and $s\bar{\mathbf{p}}$ represents the live load, s being the multiplier of the reference live load $\bar{\mathbf{p}}$.

Among the three-dimensional stress fields in equilibrium with the prescribed loads, only plane fields are considered. The out-of-plane stress component σ_3 is induced by smooth boundaries which represent the effects of either the spandrel walls or the tie rods inserted in the fill and connecting the opposite spandrel walls to strengthen masonry bridges [15]. A simple description of the stress field in arch barrels and piers is obtained by ignoring the membrane and shear forces and the bending moment acting on planes parallel to the longitudinal cross section and the twisting moment as well.

Both fill and masonry arches and piers are assumed made of no-tension rigid perfectly plastic materials. Fill is assumed as a Mohr-Coulomb cohesive-frictional no-tension material. A constraint on transverse stress is assumed $0 \ge \sigma_3 \ge -\tilde{\sigma}_c$, where the limiting value $\tilde{\sigma}_c\ (\ge 0)$ can represent either the prescribed maximum allowable pressure on the spandrel walls or the maximum allowable tensile strength of the tie rods per unit area.

The resulting conditions of plastic admissibility [14] are expressed in the form

$$\left|\sigma_1-\sigma_2\right|+\left(\sigma_1+\sigma_2\right)\sin\varphi-2c\cos\varphi\le 0\,,\quad \sigma_\alpha\le 0\,,\quad -\sigma_\alpha+\sigma_c^*-r\tilde{\sigma}_c\le 0\,,\quad \alpha=1,2\,, \qquad (1)(2)(3)$$

$\sigma_c^*=-2c\cos\varphi/(1-\sin\varphi)$ and $\sigma_t^*=2c\cos\varphi/(1+\sin\varphi)$ being the uniaxial compressive and tensile strength, respectively, and $r=-\sigma_c^*/\sigma_t^*=(1+\sin\varphi)/(1-\sin\varphi)$. The admissible range of σ_3 is obtained *a posteriori* [14] as a function of σ_1 and σ_2; the corresponding minimum admissible compressive value is

$$\text{(a) if}\quad \min\left(\sigma_\alpha,\alpha=1,2\right)\ge\sigma_c^*,\ \text{then}\ \sigma_3=0\,;\ \text{(b) else}\ \sigma_3=\sigma_t^*+1/r\ \min\left(\sigma_\alpha,\ \alpha=1,2\right). \qquad (4)(5)$$

The yield function of the cross sections of arch barrels and piers is obtained by assuming vanishing tensile strength across the mortar joints orthogonal to the centre line and rigid-ideal plastic response under compression. Sliding failure is neglected.

3. FINITE ELEMENT EQUILIBRIUM MODEL

The estimates of the collapse load multiplier s_c of the model are obtained by a finite element application of the Lower Bound Theorem of Limit Analysis. The fill is approximated by three-node triangular elements and stress discontinuities are allowed at their shared edges [16]; arches and piers are approximated by straight beam elements (Fig. 2). The presence of the discontinuities allows for enriching the stress field.

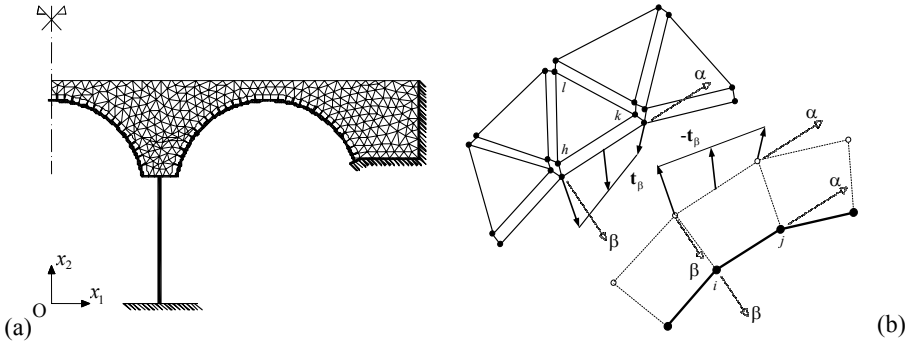

Fig. 2. (a) Finite element model of the bridge; (b) the finite element equilibrium model: arch-fill interaction tractions.

The stress field in triangular elements is assumed linearly dependent on the nodal stresses, so that the in-plane differential equilibrium equations of the *t*-th element are expressed as linear equations of the nodal stresses in the matrix form $\mathbf{C}_t^h\boldsymbol{\sigma}^h + \mathbf{C}_t^k\boldsymbol{\sigma}^k + \mathbf{C}_t^l\boldsymbol{\sigma}^l + \mathbf{c}_t = \mathbf{0}$, where the vector $\mathbf{c}_t$ depends on the applied load.

In order to preserve the lower bound property of the result, the conditions of plastic admissibility (1)-(3) are piecewise linearized in the space of stress components by an internal polyhedron obtained as intersection of three polytopes with an even number p_t of faces. The corresponding $p_f = 3p_t$ inequalities are collected in matrix form and imposed at nodes, $\mathbf{f}_t(\boldsymbol{\sigma}^r) = \mathbf{N}^T\boldsymbol{\sigma}^r - \mathbf{r}_t \le \mathbf{0}$, $r=h,k,l$.

Arches and piers are discretized by two-node straight beam elements having constant section height h and self-weight per unit length $\mathbf{b}_b$. Each beam element discretizing the arches interacts with the edge of a triangular element of fill (Fig. 2b); the generalized forces acting on the beam axis are then obtained by simply taking into account the effect of the beam height on the bending moment. The linearity of the actions coming from the fill allows for writing the overall equilibrium equations of the beam in the matrix form $\mathbf{C}_b^i\mathbf{s}_b^i + \mathbf{C}_b^j\mathbf{s}_b^j + \mathbf{C}_b^h\boldsymbol{\sigma}^h + \mathbf{C}_b^k\boldsymbol{\sigma}^k + \mathbf{c}_b = \mathbf{0}$, where $\boldsymbol{\sigma}^h$ and $\boldsymbol{\sigma}^k$ are the nodal stresses of the edge of the triangular element and vector $\mathbf{c}_b$ depends on the applied body force $\mathbf{b}_b$ (see Fig. 2b).

To obtain a linear formulation, the plastic limit envelope in the (N,M) plane is piecewise linearised by an internal polygon and imposed at a discrete number p_s ($p_s \ge 2$) of sections. The latter approximation allows a violation of equilibrium between the discrete sections that can be checked a posteriori; however, with the mesh refinement necessary for a good description of fill, the effect of this approximation was negligible even assuming $p_s \ge 2$ in the examples shown in the next section.

The generalized nodal stresses in the triangular and beam elements, collected in vector $\boldsymbol{\sigma}$, and the load multiplier s are the discrete variables which define the finite element equilibrium model. The equilibrium equations are collected in the linear matrix equation $\mathbf{C}\boldsymbol{\sigma} = \mathbf{c}$. The boundary conditions on the nodes where active and reactive forces are applied are expressed in the linear form $\mathbf{Q}\boldsymbol{\sigma} - s\bar{\mathbf{q}} = \mathbf{q}_0$, where $\mathbf{q}_0$ and $s\bar{\mathbf{q}}$ are the nodal stress vectors depending on the applied dead and live loads, respectively. Finally, the conditions of plastic admissibility are collected in the matrix inequality $\mathbf{f} = \mathbf{N}^T\boldsymbol{\sigma} - \mathbf{r} \le \mathbf{0}$. The largest lower bound s_{lb} on the collapse load multiplier is obtained as the solution of the Linear Programming problem.

$$\begin{cases} s_{lb} = \min\left(\mathbf{c}^T\boldsymbol{\alpha}_1 + \mathbf{q}_0^T\boldsymbol{\alpha}_2 + \mathbf{r}^T\boldsymbol{\alpha}_3\right), \\ \mathbf{C}^T\boldsymbol{\alpha}_1 + \mathbf{Q}^T\boldsymbol{\alpha}_2 + \mathbf{N}\boldsymbol{\alpha}_3 = \mathbf{0}, \\ \bar{\mathbf{q}}^T\boldsymbol{\alpha}_2 = 1, \\ \boldsymbol{\alpha}_3 \geq \mathbf{0}. \end{cases} \tag{6}$$

4. EXAMPLE OF APPLICATION:PRESTWOOD BRIDGE

The first example refers to Prestwood bridge, a single span bridge tested up to collapse [17] within the experimental research on masonry bridges supported by the Transport Research Laboratory (TRL). The geometry of the bridge and the position of the live load are described in Figure 3.a. The experimental arch collapse mechanism exhibits four hinges; the mechanism takes place with negligible material crushing and the experimental collapse load is $P_{exp} = 228\text{kN}$.

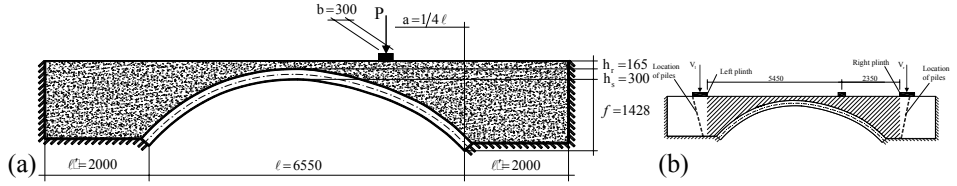

Fig. 3. (a) Prestwood bridge model (mm). (b) Position (mm) of the plinths of the loading system and of the piles at abutments.

Figure 4 shows the numerical results obtained by assuming plane strain fill and the mechanical parameters given in Table 1; the values of the angle of internal friction φ and the compressive masonry strength σ_c come from experimental evaluations [17], while data about cohesion c furnished in [17] are not sufficient and the assumed value is such that the experimental collapse load $P_{exp} = 228\text{kN}$ is approximately the average between the equilibrium ($P^{lb}_{strain} = 209\text{kN}$) and the compatible ($P^{ub}_{strain} = 254\text{kN}$) solutions. An analysis of the sensitivity of the results on the mechanical parameters has been carried out and will be discussed shortly.

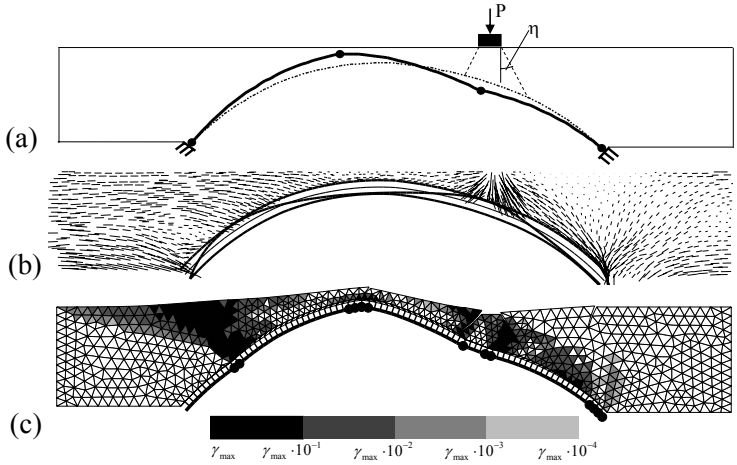

Fig. 4. (a) Collapse mechanism with non resistant fill ($P_{nrf} = 46.2\text{kN}$); (b) in-plane principal stress field and line of thrust (plane strain fill) ($P^{lb}_{strain} = 208.8\text{kN}$); (c) collapse mechanism and contour plot of the maximum shear strain rate from compatible model (plane strain fill) ($P^{ub}_{strain} = 254.5\text{kN}$).

Table 1 Prestwood bridge: constitutive parameters; experimental and numerical collapse loads.

Masonry density	γ_m	$20\,kN/m^3$	*Exp. collapse load*	P_{exp}	228kN
Masonry compr. strength	σ_c	4.5MPa	*Non res. fill coll. load*	P_{nrf}	46kN
Fill density	γ_f	$20\,kN/m^3$	*Plane strain lb*	P^{lb}_{strain}	209kN
Angle of int. friction	φ	37^o	*Plane strain ub*	P^{ub}_{strain}	254kN

Figure 4.a shows the collapse mechanism obtained by assuming heavy but non resistant fill and distributing the live load on the arch by assuming $\eta = 30^o$; the dark circles in the arch are the generalised hinges. The corresponding collapse load is $P_{nrf} = 46kN$ and agrees with the result obtained by Crisfield [9]. The limit stress state and the collapse mechanism [13] obtained by assuming plane strain fill are shown in Figure 4.b and 4.c, respectively. In Figure 4.b the thick line in the depth of the arch represents the thrust line, while the straight lines in the fill represent the principal directions of the stress field; the contour plot in the fill in Figure 4.c shows the maximum shear strain rate field. A good qualitative agreement between the results from the equilibrium and compatible models is obtained. The limit state described by the numerical results appears to well reproduce the experimental behaviour; in particular, the location of the hinges from the analysis are a good approximation of the experimental positions.

The contour plot of the minimum compressive stress field σ_3 is shown in Figure 5. The minimum values are reached in small regions located below the live load and at springings; the in-plane stress field in the regions in white is compatible with plane stress fill.

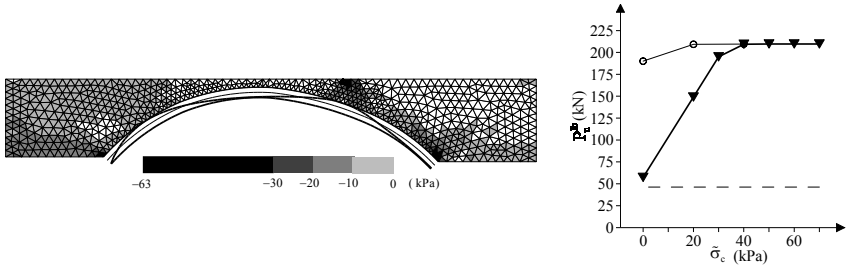

Fig. 5. (a) Contour plot of the minimum compressive stress σ_3 .(b) Influence of the allowable transverse stress $\tilde{\sigma}_c$ on the lower estimates of collapse load (bold line); estimates obtained by imposing plain strain under the punch (thin line); estimates obtained by assuming heavy non resistant fill (dashed line).

The effects of the maximum allowable transverse stress $\tilde{\sigma}_c$ on the lower estimates of the collapse load are shown in the graph of Figure 5b (bold line). For $\tilde{\sigma}_c \geq 63kPa$ the plane strain limit stress state is obtained; for $\tilde{\sigma}_c < 63kPa$ the out of plane limit condition affects the result until the value $P^{lb}_{stress} = 57kN$ obtained by assuming $\tilde{\sigma}_c = 0kPa$ (plane stress).

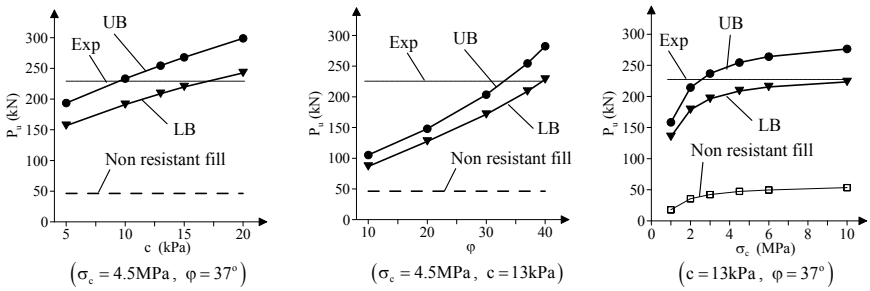

Fig. 6. Effects (a) of the cohesion c, (b) of the angle of internal friction φ and (c) of masonry compressive strength σ_c .

The equilibrium solution corresponding to $\tilde{\sigma}_c = 20\text{kPa}$ is $P_u^{lb} = 149\text{kN}$ and the stress field, not shown, is similar to the case of plane strain fill, with lower values of σ_3. The limit state due to the limitation of the transverse stress σ_3 is first reached just under the live load, so that the load is equilibrated by a uniform distribution of the maximum compressive stress $\sigma_c^* - r\tilde{\sigma}_c$. The decreased estimate of the collapse load is therefore due to a local effect; this aspect is well shown by the results obtained by keeping the cone under the live load in plane strain and varying $\tilde{\sigma}_c$ through the rest of the fill; the lower bound on the collapse load (Figure 5b, thin line) decreases only for very low values of $\tilde{\sigma}_c$.

The effects of the cohesion c and the angle of friction φ of the fill on the lower and upper bound estimates of collapse load by assuming plane strain are shown in the graphs of Figure 6.a and 6.b, respectively; the effect of the masonry compressive strength σ_c is shown in Figure 6.c. The contribution of the fill resistance to the collapse load estimates is important also for low values of cohesion and friction. The effects of a decrease in the cohesion are limited, and the lower estimate of the collapse load is still higher than 150 kN by assuming $c = 5\text{kPa}$. Finally, the effects of the masonry compressive strength σ_c are negligible only for $\sigma_c \geq 6$ MPa.

The particular procedure followed to apply the load during the experimental test [17] makes it necessary to evaluate its possible effects on the results. Dead load to provide reaction for the jacks was provided by concrete blocks supported above the bridge by three beams resting on concrete bolck plinths at each abutment (Fig. 3.b). The vertical forces V_l and V_r (Figure 3.b) applied on the fill depend on the weight of the concrete blocks (380kN) and the supporting structure and on the force exerted by the jacks. The results obtained by introducing these forces in the numerical simulation have shown that their effect is negligible. The analysis has shown that only large increments of the weight of the loading system can significantly affect the results.

Finally, an analysis of the effect of the fill constrains at the abutments has been carried out by considering a reduced domain of the fill, corresponding to the shaded region in Figure 3.b. Also in this case, the differences in the compatible and equilibrium solutions provided by the model in plain strain condition with respect to the results obtained by the reference one are less than 1%. This results shows that, for this particular load condition, the introduction in the simulation of the piles present at the abutments would not have affected the results.

5. CONCLUSION

A two-dimensional statically admissible finite element model and a numerical procedure have been presented to analyse the collapse behavior of masonry bridges taking into account the interaction between the arch-pier structural system and fill.. The effects of a limited transverse strength of spandrel walls on fill and, as a consequence, on collapse load are taken into account by introducing a simplified condition that limits the transverse compressive stress in the fill.

The procedure has been applied to simulate an experimental collapse test [17] that allowed for a comparison between the numerical and experimental results. The results obtained by varying the admissible transverse stress have highlighted the important influence of this parameter on the collapse load and the validity limits of the plane strain assumption.

AKNOWLEDGEMENTS

The authors acknowledge financial support of the (MURST) Italian Department for University and Scientific and Technological Research in the frame of the research project PRIN 2003/ 2004 Project "*Safety, maintenance and management of Masonry Bridges*".

REFERENCES

[1] Page J., Masonry Arch Bridges - TRL State of the Art Review, HMSO, 1993.
[2] Fanning P. J., Boothby T.E., Three-dimensional modelling and full-scale testing of stone arch bridges, *Computers and Structures*, **79**, 2645-2662, 2001.

[3] Castigliano C.A.P., Theorie de l'equilibre des systemes elastiques et ses applications, Augusto Federico Negro, Torino, 1879; Andrews E.S., Elastic stresses in structures. Translation by Andrews, Scott Greenwood & Son, London, 1919.
[4] Kooharian A., Limit analysis of voussoir (segmental) and concrete arches, *Proc. Am. Concr. Inst.*, **89**, 317-328, 1953.
[5] Heyman J., The stone skeleton, *Int. J. Solids Structures*, **2**, 249-279, 1966.
[6] Crisfield M.A., Finite element and mechanism methods for the analysis of masonry and brickwork arches, Transport Research Laboratory, Crowthorne, Research Report 19, 1985.
[7] Choo B. S., Coutie M. G., Gong N. G., Finite element analysis of masonry arch bridges using tapered elements, *Proc. Instn. Civ. Engrs.*, Part 2, **91**, Dec. 755-770, 1991.
[8] Crisfield M.A., Packam A. J., A mechanism program for computing the strength of masonry arch bridges. Transport Research Laboratory, Crowthorne, Research Report 124, 1985.
[9] Hughes T.G., Hee S. C., Soms E., Mechanism analysis of single span masonry arch bridges using a spreadsheet, *Proc.Inst. Civ. Eng. Struct. Build.,* **152**, 341-350, 2002.
[10] Bicanić N., Ponniah D., Robinson J., Discontinuous deformation analysis of masonry bridges, *Computational Modelling of Masonry, Brickwork and Blockwork Structures*, J.W. Bull Ed., 177-196, Saxe-Coburg Publications, Stirling, 2001.
[11] Cavicchi A., Analisi limite agli elementi finiti di archi murari interagenti con il riempimento per la valutazione della capacità portante di ponti in muratura, Ph.D. Thesis, Department of Structural and Geotechnical Engineering, University of Genova, Italy, 2004 (in Italian).
[12] Cavicchi A., Gambarotta L, Collapse analysis of masonry bridges taking into account arch-fill interaction, *Engineering Structures*, 27, 605-615, 2005.
[13] Cavicchi A., Gambarotta L, Two-dimensional upper bound limit analysis of masonry bridges, *Computers & Structures*, 84, 2316-2328, 2006.
[14] Cavicchi A., Gambarotta L, Lower bound limit analysis of masonry bridges including arch-fill interaction, *Engineering Structures*, to appear, 2007.
[15] Oliveira D.V., Lourenco P.B., Repair of stone masonry arch bridges, *Proc. Arch Bridges ARCH '04*, Barcelona, 451-458, 2004.
[16] Sloan S.W., Lower bound limit analysis using finite elements and linear programming, *Int. J. Numerical and Analytical Methods in Geomechanics*, 12, 61-77, 1988.
[17] Page J., Load tests to collapse on two arch bridges at Preston, Shropshire and Prestwood, Staffordshire, Department of Transport, TRRL Research Report 110, TRL, Crowthorne, England, 1987.